17th Brazilian Congress of Thermal Sciences and Engineering
November 25th-28th, 2018, Águas de Lindóia, SP, Brazil

ENCIT-2018-0107
NUMERICAL ANALYSIS OF A GENERIC SCRAMJET AIR INLET

Paulo Gilberto de Paula Toro
Jonatha Wallace da Silva Araújo
Emanuel Vieira Mendes
Sandi Itamar Schafer de Souza
Universidade Federal do Rio Grande do Norte/UFRN - Centro de Tecnologia. Av. Senador Salgado Filho, 3000 - Campus Universitário, Lagoa Nova CEP 59.078-970 – Natal/RN - Brasil
toro@ct.ufrn.br; jonatha_wallace@hotmail.com; emanuel-mendes@hotmail.com; sandi@ufrnet.br

Israel da Silveira Rêgo
Instituto de Estudos Avançados/IEAv - Trevo Coronel Aviador José Alberto Albano do Amarante, nº1 Putim CEP. 12.228-001 São José dos Campos, SP - Brasil
israel.rego@ieav.ct.br

Abstract. *A generic hypersonic airbreathing propulsion based on supersonic combustion ramjet (scramjet) technology has been designed, at the Universidade Federal do Rio Grande do Norte (UFRN), using both analytical and numerical theoretical analysis. The scramjet will demonstrate supersonic combustion during Earth's atmospheric free-flight at 30 km of geometric altitude and Mach number 6.8. Plane oblique shock wave (two-dimensional steady state, non-viscous, adiabatic calorically compressible airflow) is used for analytical theoretical analysis. Fluent software has been applied for the (Computational Fluid Dynamics) numerical simulation considering non-viscous calorically airflow for the scramjet inlet. Implicit second order upwind spatial discretization is used to obtain the contour plots of the static pressure, temperature, density and airflow velocity (and corresponding Mach number). Numerical simulation of the above quantities at the scramjet inlet are compared to the analytical theoretical results based on the plane oblique shock wave theory.*

Keywords: *scramjet, supersonic combustion ramjet, hypersonic airbreathing propulsion, numerical simulation.*

1. INTRODUCTION

In 2012, Brazilian researchers, from Laboratório de Aerotermodinâmica e Hipersônica Prof. Henry T. Nagamatsu, at Instituto de Estudos Avançados (IEAv), proposed to design, to develop, to manufacture and to demonstrate, in free flight, a technological demonstrator using scramjet technology to provide hypersonic airbreathing propulsion system based on supersonic combustion.

The fully airframe-integrated scramjet 14-X S (Fig. 1) is being designed to demonstrate supersonic combustion during atmospheric flight in 7 (approximately 2100 m/s).

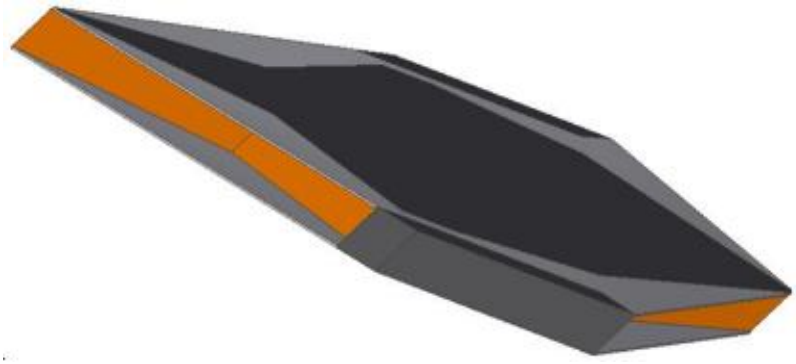

Figure 1. Demonstrator scramjet 14-X S.

The original 14-X S consists a two-dimensional configuration (Fig. 1), with a constant cross-section (Fig. 2), which shows only the half of the constant cross-section. The scramjet surface consists of a frontal surface with a leading edge

angle of 5.5^o, compression ramp angle of 14.5^o (related to the angle of the leading edge), the internal expansion chamber combustion angle of 4.27^o and external expansion angle of 10.73^o (related to the angle of internal expansion).

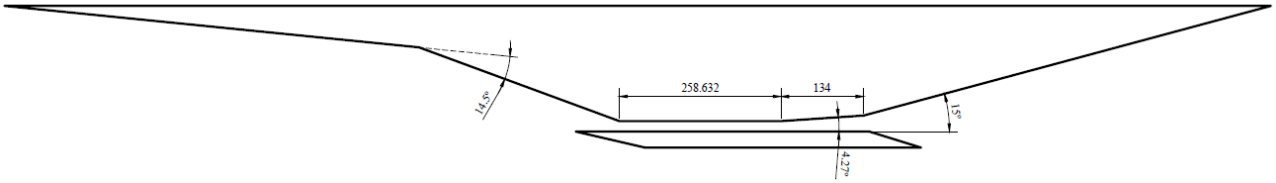

Figure 2. Cross-section of the 14-X S (with two compression ramps) flying at 30km altitude at Mach number 7.

Martos et al. (2017) developed experimental investigation at T3 Hypersonic Shock Tunnel (Fig. 3), where the half of the 14-X S model (Fig. 2) was scaled based on the 14-X S hypersonic scramjet aerospace vehicle design for flight at Mach number 7 and 30 km of altitude (Fig. 1). The model inlet (Fig. 4) consists of a two-dimensional configuration, with a constant cross-section, where the upper flat surface, with zero angle of attack, is aligned with the freestream Mach number 7 hypersonic airflow.

Figura 3. Hypersonic Shock Tunnel T3 (Romanelli Pinto et al, 2011).

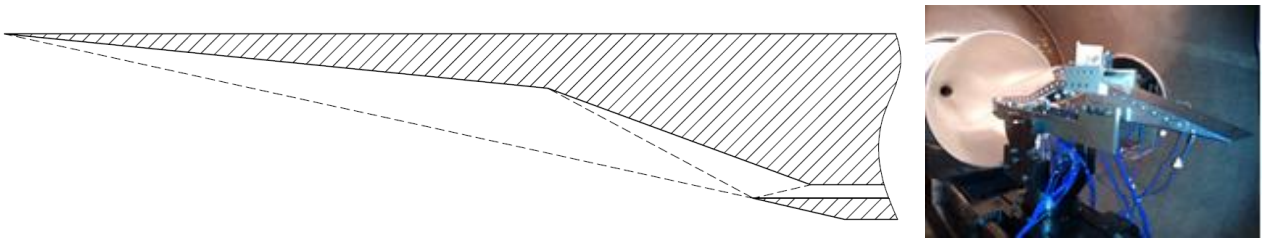

(a) (b)

Figure 4. (a) Half of the 14-X S model. (b) installed model in the T3 test section of the T3 Hypersonic Shock Tunnel

In the Martos et al. (2013) experimental investigations was observed the boundary layer and shock wave interaction between first and second ramp of the inlet (Fig. 5). According to Heiser and Pratt (1994) for Mach 7 the maximum angle between these two ramps should be around 12º to minimize the boundary layer separation. The separation of the boundary layer is critical for a hypersonic inlet because it changes shock wave angle, pressure recovery, and heat transfer while may lead to chocked flow even resulting in unstart of the engine. The half of the 14-X S model has a turning angle of 14.5º between its compression ramps, such that for some experimental conditions were possible to observe the separation of the boundary layer but not the reattachment of it.

To assure the reattachment of the boundary layer and to minimize the boundary layer and shock wave interaction effects a new version of the 14-X S with three ramps was designed to fly at a Mach number $M = 7$ through Earth's

Atmosphere ($\gamma = 1.4$) at 30 km geometric altitude. The scramjet inlet consists of three with the attached incident oblique shockwave angle at the leading-edge of 5.5° (to be consistent with the leading-edge of the scramjet 14-X S with two ramps, and the incident oblique shockwave angles establish at the corner of the compression ramps of 7° and 8.5° (Fig. 5).

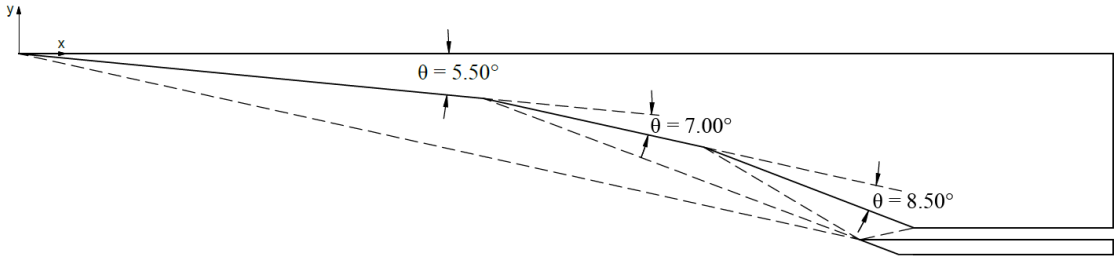

Figure 5. Cross section of the generic scramjet inlet.

2. METHODOLOGY

2.1 Scramjet characteristics

First, it is necessary to establish a nomenclature to be used in the scramjet design. Heiser and Pratt (1994) present the terminology of the scramjet, which may be divided in three main components (Fig. 6): external and internal compression section (inlet), combustion chamber (combustor), and internal and external expansion section (outlet).

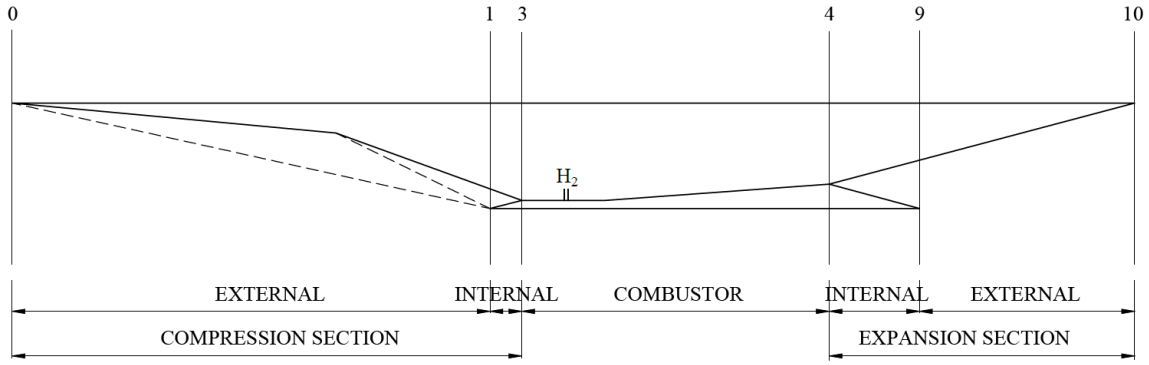

Figure 6. Airframe-integrated scramjet engine stations and reference terminology (adapted from Heiser and Pratt, 1994).

Stations 0 and 1 are the leading edges of the scramjet and of the cowl, respectively. Stations 3 and 4 are the entrance and exit of the combustion chamber. Stations 9 and 10 are the trailing edges of the cowl and the scramjet, respectively.

The external compression section is governed by incident shock wave, while the internal is governed by reflected shock wave. The internal and external expansion section is governed by expansion wave, Prandtl-Meyer Theory, and area ratio. The constant area section of the combustion chamber is called as isolator and is used to uniformize the flow from the compression section. Fuel is injected right after the isolator used to expand the gases from burning the fuel and the oxygen. In general, one-dimensional flow with heat addition, Rayleigh flow, is used to simulate the burning the fuel and the oxygen.

An important feature of the scramjet is a highly integrated system, where engine and vehicle are indistinguishable. This tight integration is caused by the fact that the front section of the vehicle contributes to the compression of atmospheric air, while the rear contributes to the generation of thrust. The net thrust produced by the scramjet is the difference between the thrust (force that propels the vehicle) generated by the expansion of exhaust gases from the rear of the engine and the total drag (force that resists the movement of the vehicle). These forces may produce thrust to the flight of the vehicle or not depending on the balance of these forces in engine design in question.

2.2 Governing conservation laws (plane oblique shock wave theory)

In the analytical theoretical analysis, the subscripts *in* and *out* are used to identify the upstream (inlet) and the downstream (outlet) conditions, respectively, of each station (Fig. 7) of the generic scramjet inlet baseline.

Considering mass, momentum and energy conservation laws in two-dimensional steady state, compressible flow, applied to plane oblique shock wave (Anderson, 1990) with no boundary-layer effects (inviscid flow), no heat conduction and calorically perfect gas ($p = \rho RT$, $\gamma = \text{constant}$) the shock wave angle β (Fig. 7) is a function of the incoming local supersonic/hypersonic flow Mach number M_{in}, the gas from the atmosphere γ (air in the Earth's planet, $\gamma = 1.4$) and the deflection angle θ_s , and it may be obtained iteratively with the relationship given by:

$$tg\theta_s = 2(\text{cotg}\,\beta)\left[\frac{\left(M_{in}\ sen\beta\right)^2 - 1}{M_{in}^2(\gamma + \cos 2\beta) + 2}\right] \tag{1}$$

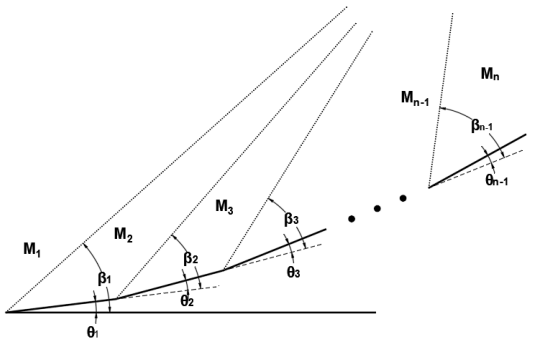

Figure 7. Incident and reflected oblique shockwave geometries.

where: ρ , p , u_{1n} , u_{1t} , h are density, pressure, normal and tangential velocities across the plane oblique shock wave and enthalpy of the gas, respectively.

Additionally, the oblique shock relationships can be easily obtained as closed form of the thermodynamic property (static pressure, static density, static temperature, …) ratios and Mach number across the oblique shock given by:

$$\frac{p_{out}}{p_{in}} = 1 + \frac{2\gamma}{(\gamma+1)}\left[\left(M_{in}\ sen\beta\right)^2 - 1\right] \tag{2}$$

$$\frac{\rho_{out}}{\rho_{in}} = \frac{(\gamma+1)\left(M_{in}\ sen\beta\right)^2}{\left[(\gamma-1)\left(M_{in}\ sen\beta\right)^2 + 2\right]} \tag{3}$$

$$\frac{T_{out}}{T_{in}} = \frac{p_{out}}{p_{in}}\ \frac{\rho_{in}}{\rho_{out}} = 1 + \frac{2\gamma}{(\gamma+1)}\left[\left(M_{in}\ sen\beta\right)^2 - 1\right]\ \frac{\left[(\gamma-1)\left(M_{in}\ sen\beta\right)^2 + 2\right]}{(\gamma+1)\left(M_{in}\ sen\beta\right)^2} \tag{4}$$

$$M_{out} = \frac{\sqrt{\dfrac{\left(M_{in}\ sen\beta\right)^2 + \dfrac{2}{(\gamma-1)}}{\dfrac{2\gamma}{(\gamma-1)}\left(M_{in}\ sen\beta\right)^2 - 1}}}{sen\left(\beta - \theta_s\right)} \tag{5}$$

Note, the flow across the plane oblique shock wave promote an increase of pressure, density, temperature, and a decrease of Mach number, however the flow remains supersonic/hypersonic and parallel to the flat surface of the external compression section (Fig. 7) of the hypersonic vehicle with airframe-integrated scramjet engine lower surface.

Also, the leading-edge incident plane oblique shock wave theory may be used for incident oblique planar (Fig. 8) shock wave (compression ramp angle) and the reflected shock wave (Fig. 7).

2.3 Governing conservation laws (Computational Fluid Dynamic theory)

The "Fluent" software solves Navier-Stokes equations (mass, momentum and energy conservation equations), which are valid for continuum media, considers reacting flow and includes routines (solvers) that accurately simulate the

behavior of flow, single phase and multiphase, Newtonian and non-Newtonian flow from subsonic to hypersonic speed, is able to perform a numerical theoretical simulation applied to the Brazilian technological demonstrators.

The Navier-Stokes equations, in 2-D, are given by

$$\frac{\partial U}{\partial t}+\frac{\partial E}{\partial x}+\frac{\partial F}{\partial y}=0 \tag{6}$$

where U is a solution column vector, E and F are flux terms column vectors, given by

$$U=\begin{Bmatrix}\rho\\ \rho u\\ \rho v\\ E_t\end{Bmatrix} \qquad E=\begin{Bmatrix}\rho u\\ \rho uu+p-\tau_{xx}\\ \rho uv-\tau_{xy}\\ (E_t+p)u+q_x-u\tau_{xx}-v\tau_{xy}\end{Bmatrix} \quad F=\begin{Bmatrix}\rho v\\ \rho vu-\tau_{yx}\\ \rho vv+p-\tau_{yy}\\ (E_t+p)v+q_y-u\tau_{yx}-v\tau_{yy}\end{Bmatrix} \tag{7}$$

The viscous terms and the heat flux by conduction are given by:

$$\tau_{xx}=\lambda\left(\nabla.\vec{V}\right)+2\mu\frac{\partial u}{\partial x} \qquad \tau_{yy}=\lambda\left(\nabla.\vec{V}\right)+2\mu\frac{\partial v}{\partial y} \qquad \tau_{xy}=\tau_{yx}=\mu\left(\frac{\partial u}{\partial y}+\frac{\partial v}{\partial x}\right) \tag{8}$$

$$q_x=-k\frac{\partial T}{\partial x} \qquad q_y=-k\frac{\partial T}{\partial y} \tag{9}$$

where for Newtonian fluid

$$\lambda=-\frac{2}{3}\mu \tag{10}$$

3. RESULTS AND COMMENTARIES

Analytical theoretical analysis is applied to the lower surface of the scramjet inlet, considering the simplest case, i. e., non-viscous flow, calorically perfect air $\gamma = 1.4$ (Table 1).

The $\theta-\beta-M$ relation (Eq. 1) is applied to obtain the incident oblique shockwave angles as well as the reflected oblique shockwave angle (Tab. 1). Following, the thermodynamic air properties after each event (Tab. 1) may be evaluated by the thermodynamic property ratio (Eqs. 2-4) and the freestream thermodynamic properties (Tab. 1). The Mach number after each incident and reflected shockwave may be evaluated by Eq. 5 (Tab. 1).

The cross-section dimensional geometry of the scramjet inlet (Fig. 5) may be determined assuming that: i) The scramjet (Fig. 1) is flying at 30 km geometric altitude (U.S. Standard Atmosphere, 1976), where the static pressure, static temperature, static density and sound velocity are given by p = 1197 Pa, T = 226.5 K, $\rho = 0.01841$ kg/m^3, a = 301.7 m/s, respectively at Mach number 6.8; ii) The leading-edge angle is 5.5º, following by two compression ramps with turning angles of 7º and 8.5º; iii) The incident shock waves generated at the 5.5° attached leading-edge deflection angle and at the 7° and 8.5º deflection angles (following the leading-edge deflection angle) hit the cowl leading-edge, and the reflected shock wave generated at the cowl leading-edge hits the entrance of the combustor station, therefore, the flow mass rate at the combustor inlet is the same as the flow mass rate at the frontal area of the generic scramjet.

The generic scramjet, with three ramps at the compression section (Fig. 8), with leading-edge angle of 5.5º, followed by two deflection angles of 7º and 8.5º, flying at 30 km of geometric altitude with speed corresponding at Mach number 6.8 is capable to generate a supersonic velocity corresponding to Mach number of 2.55 and a static temperature (Tab. 1) higher than 845.15 K, ignition temperature of hydrogen (Coordinating Research Council, 1983), at the entrance of combustion chamber. Consequently, it is possible to demonstrate a supersonic combustion when hydrogen may burn the supersonic atmospheric air, at the combustion chamber, during the atmospheric hypersonic flight of this generic scramjet.

Note, the supersonic airflow across the plane attached shockwave promotes an increase of thermodynamic properties (pressure, temperature, density) and a decrease of flow velocity (Mach number), and the plane streamline of the airflow remains supersonic and parallel to the flat surface (Tab. 1) of the generic scramjet starting at 5.5º leading-edge deflected

angle, as well as for the two compression ramps, with the turning angles of 7º and 8.5º, and after the reflected shock wave.

Table 1. Thermodynamic properties at the generic scramjet engine inlet, non-viscous flow, calorically perfect gas ($p = \rho RT$, $\gamma = 1.4$).

		Freestream	Ramp 5.5°	Ramp 7°	Ramp 8.5°	Reflection
M_{in}	-	6.8	6.8	5.86	4.95	4.11
θ_{in}	º	-	5.5°	7°	8.5°	21°
β_{out}	º	-	12.47	15.04	18.12	33.22
M_{out}	-	-	5.86	4.95	4.11	2.55
$\frac{p_{out}}{p_{in}}$	-	-	2.35	2.54	2.60	5.76
$\frac{T_{out}}{T_{in}}$	-	-	1.30	1.34	1.35	1.90
$\frac{\rho_{out}}{\rho_{in}}$	-	-	1.81	1.90	1.93	3.02
p_{out}	Pa	1197	2813.18	7145.42	18582.81	106991.30
T_{out}	K	226.5	294.35	393.15	529.62	1008.64
ρ_{out}	kg/m^3	0.01841	0.03329	0.06331	0.12223	0.36952
a_{out}	m/s	301.7	343.94	397.49	461.35	636.67
u_{out}	m/s	2051.6	2018.08	1928.30	1897.37	1624.01

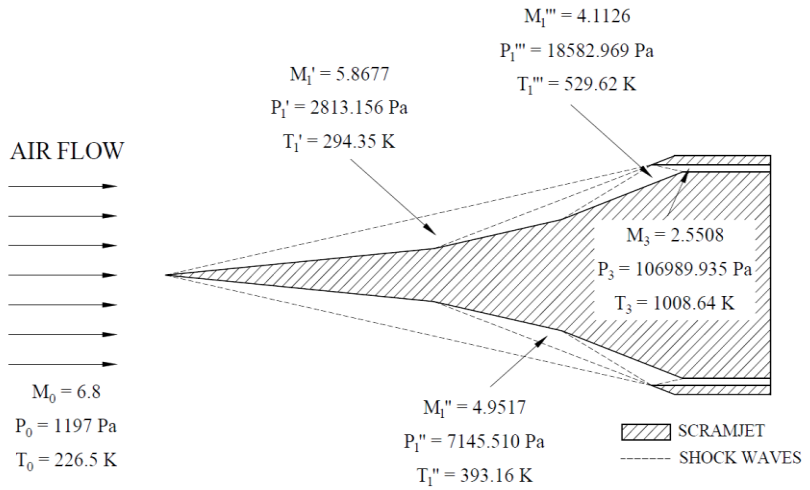

Figure 8. Thermodynamic properties at the inlet of the generic scramjet.

For the present numerical test case, with power-off scramjet engine, the flow from the (external and internal) compression section are deflected to the combustor entrance (Fig. 3) at supersonic speed with constant pressure, constant density, constant temperature and constant velocity (and corresponding Mach number) remaining constant until the exit of the combustor.

Note that, the incident oblique shock waves generated at the 5.5° attached leading-edge deflection angle as well as generated at the intersections at the 7° and the 8.5° (second and third compression ramp deflections) hit very closely the cowl leading-edge (Figs. 9 to 14) in accordance with the inlet design criteria of the 14-X S. Also, the reflected shock wave due to the incident oblique shock waves impinges very closely the entrance of the combustor.

Figures 9 to 14 show a very weak shock train at the combustor inlet entrance, suggesting that a uniform supersonic flow (constant pressure, constant density, constant temperature, constant sound speed, constant flow velocity and corresponding flow Mach number) is established at the combustor inlet.

As one may observe the airflow velocity and Mach number at the combustor chamber entrance is supersonic, higher than Mach number 2 (Figs. 9 and 10).

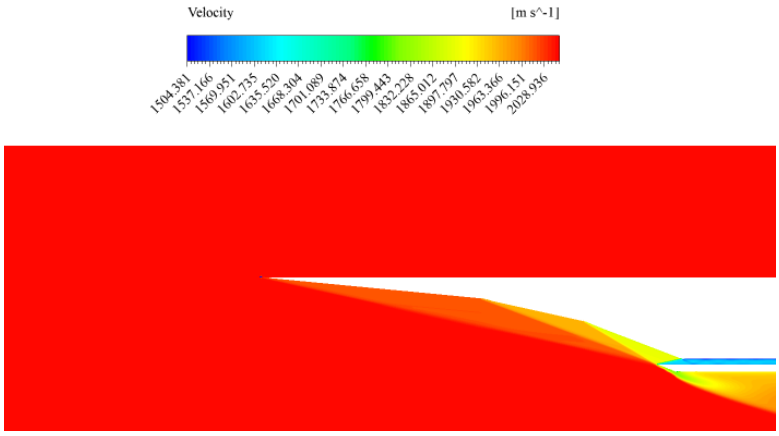

Figure 9. Airflow velocity contour plot.

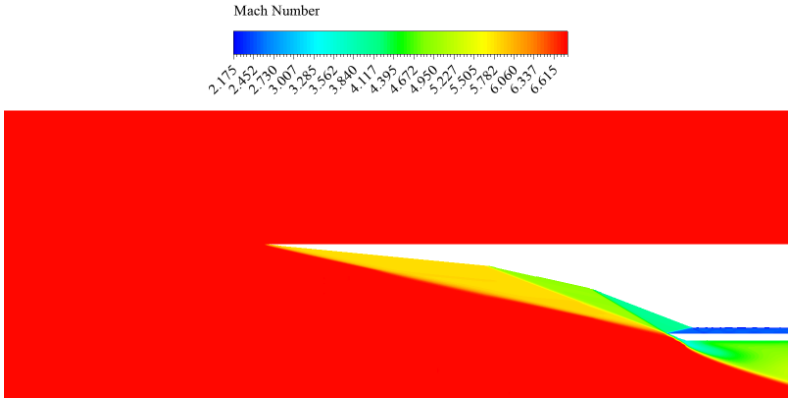

Figure 10. Airflow Mach number contour plot.

Schlieren pictures, which are based on density gradients, may be taken from the T3 Hypersonic Shock Tunnel experimental investigations of the hypersonic flight at Mach number 6.8 of this scramjet inlet and compared with the contour plot of the static density gradient across the lower surface (Fig. 11). Note that, the interaction of the hypersonic Mach number 6.8 with the 5.5° attached leading-edge deflection angle establishes a weak density gradient in comparison with the other two turning angles of 7° and 8.5°.

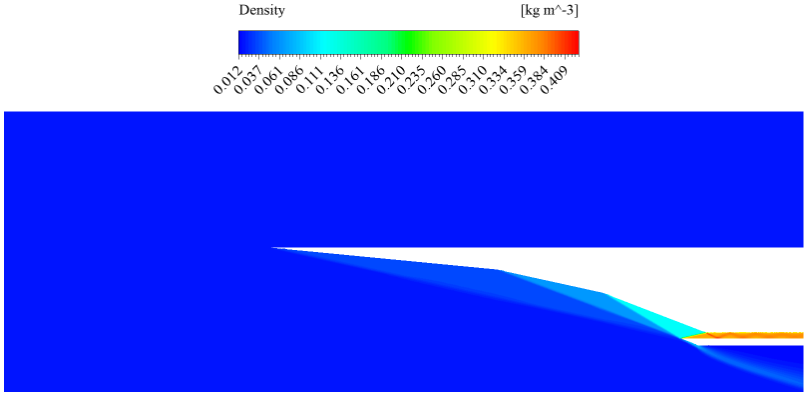

Figure 11. Contour plot of static density.

The maximum static pressure (Table 1) occurs at the combustor (Fig. 12) and may be used as a guide to specify the fuel injection layout and conditions to the static and dynamic structural analysis of the 14-X S.

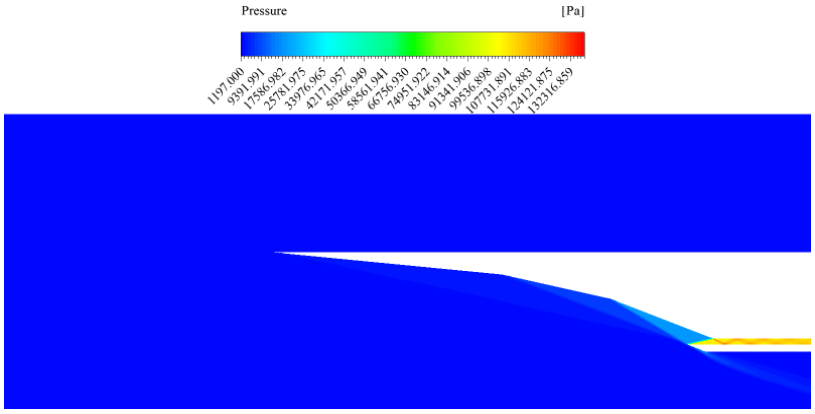

Figure 12. Contour plot of static pressure.

The scramjet air intake configuration with 5.5° leading-edge deflection angle followed by the 7° and 8.5° turning angles is capable to generate a static temperature about 1008 K (Table 1) at the combustor (Fig. 13) higher than the ignition temperature of 845 K for hydrogen (Coordinating Research Council, 1983), with supersonic Mach number higher than 2 (Table 3) at the combustor chamber. Note the sound speed (Fig. 14) accompanying the temperature of the airflow (Fig. 14).

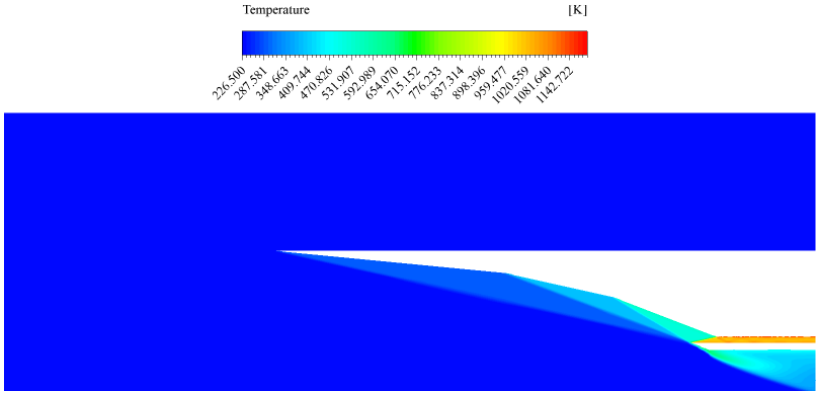

Figure 13. Contour plot of static temperature.

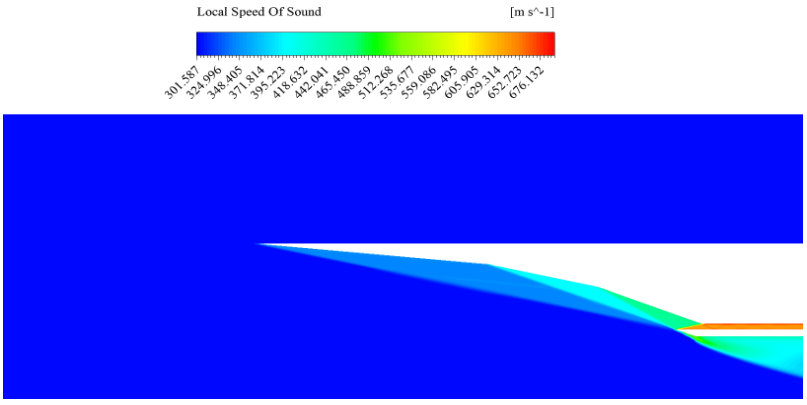

Figure 14. Contour plot of static sound speed.

Figure 15 compares the numerical pressure, temperature, density and Mach number simulation results (Figs. 9 to 14) and the analytical theoretical pressure analysis result (Table 1) both applied to the lower surface of the half of the 14-X

S. Also, the thermodynamic property distribution shows the shock train from the numerical simulation at the combustor section.

In the present work the analytical theoretical analysis and the numerical simulations are based on the perfect gas and inviscid flow assumptions, therefore the results must be the same.

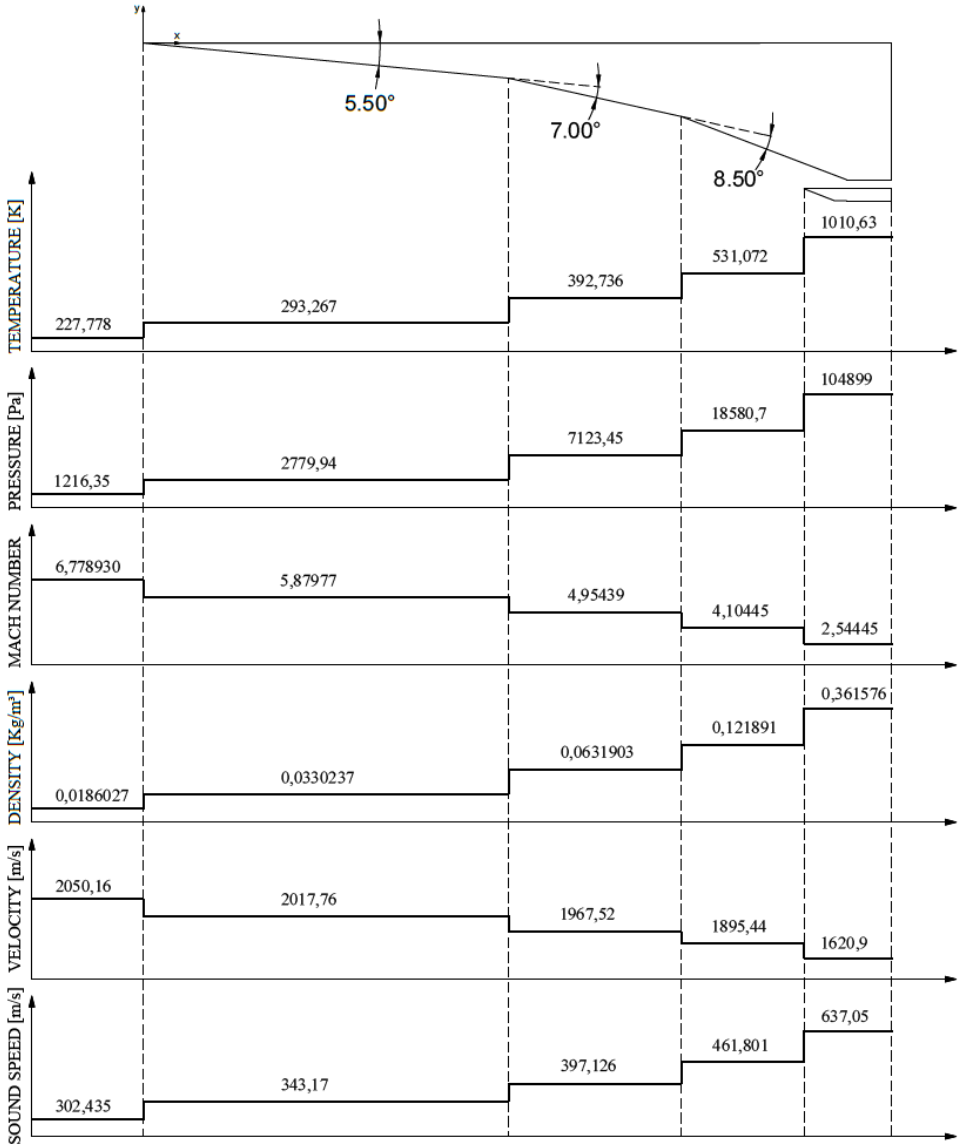

Figure 15. Numerical thermodynamic property distribution along of the scramjet inlet.

4. CONCLUSION AND OUTLOOK FOR FUTURE PROJECTS

The primary objective of this work is to present the numerical simulation of the inlet of the generic scramjet, corresponding to the scramjet 14-X S with three compression ramps, which is designed as an option of a new generation of scientific aerospace vehicle to replace not in a too distant future the conventional multi-stage rocket-powered vehicles, which have flown hypersonically, carrying their own propellant (solid and/or liquid, oxidizer along with fuel) to propel payloads and astronauts to Earth's orbit.

The Brazilian 14-X S, designed at the Prof. Henry T. Nagamatsu Laboratory of Aerothermodynamics and Hypersonics, is part of the continuing effort of the Department of Aerospace Science and Technology (DCTA), to develop a technologic demonstrator for flying at 30 km of altitude and Mach number 7, using "scramjet" technology to provide hypersonic airbreathing propulsion system based on supersonic combustion.

Basically, scramjet is a fully integrated airbreathing aeronautical engine that uses the oblique/conical shock waves generated during the hypersonic flight, to promote compression and deceleration of freestream atmospheric air before getting into the combustor of the scramjet.

Analytical theoretical analysis, computational fluid dynamics simulation and experimental investigation are the methodologies used to design the Brazilians technological demonstrators, before flying through Earth's atmosphere.

Two-dimensional steady state, non-viscous, adiabatic compressible flow applied to airflow across the shock and expansion waves may be used as analytical theoretical analysis.

Fluent commercial code has been applied for the numerical simulation considering non-viscous calorically airflow for the scramjet inlet, that should be used at the 14-X S to fly at 30 km of altitude and Mach number 6.8. Implicit second order upwind spatial discretization is used to obtain the distributions of the static pressure, temperature and density and Mach number.

Numerical simulation results are comparable to the analytical theoretical analysis results applied to the scramjet inlet. The very weak shock train established at the combustor section shows the uniformity of the static pressure, static temperature, static density and Mach number. Also, the level of the temperature about 1000 K at the combustor inlet is enough to burn the hydrogen fuel without any igniter.

5. ACKNOWLEDGEMENTS

The first four authors would like to thanks to Universidade Federal do Rio Grande do Norte (UFRN) the support given to complete this scientific work. The first author (as Visiting Professor) would like to express appreciation to UFRN the possibility to apply the knowledge in aerothermodynamics and hypersonics in the research area in hypersonic airbreathing propulsion based on supersonic combustion ramjet (scramjet) technology. Finally, a portion of this effort was supported by Instituto de Estudos Avançados (IEAv) and by the Propulsão Hipersônica 14-X (PropHiper) Project and the last author would like express his appreciation.

6. REFERENCES

Anderson, J. D., Modern Compressible Flow, The Historical Perspective. McGraw-Hill, Inc., ed. 2nd, 1990.

Coordinating Research Council, Inc. "Aviation Fuel Properties". CRC Report No. 530, September 1983.

Romanelli Pinto, D.; Marcos, T.V.C.; Galvao, V.A.B.; Oliveira, A.C.; Chanes Jr, J.B.; Minucci, M.A.S.; Toro, P.G.P. Toro, Flow Characterization of the T3 Hypersonic Shock Tunnel, In: 28th International Symposium on Shock Waves, 2011.

Heiser, W. H.; Pratt, D. T. Hypersonic Airbreathing Propulsion. Washington, D.C, American Institute of Aeronautics and Astronautics, 1994.

Martos, J. F. A. Aerothermodynamic design, manufacturing and testing of a 3-d prototyped scramjet. Thesis of Doctor in Science - Space Science and Technology, Space Propulsion and Hypersonics – Instituto Tecnológico de Aeronáutica, 2017.

U.S. Standard Atmosphere. NASA TM-X 74335. National Oceanic and Atmospheric Administration, National Aeronautics and Space Administration and United States Air Force. 1976.

7. RESPONSIBILITY NOTICE

The authors are the only responsible for the printed material included in this scientific article.

The authors declare that there is no conflict of interest regarding the publication of this scientific article.